

Site determination of radioactive atoms from the interference effect of electron-capture x rays

Yuji C. Sasaki, Yoshio Suzuki, Yasushi Tomioka, and Tadashi Ishibashi
Advanced Research Laboratory, Hitachi Ltd., Hatoyama, Saitama, 350-03, Japan

Isamu Satoh and Kichinosuke Hirokawa

Institute for Materials Research, Tohoku University, 2-1-1 Katahira, Aoba-ku, Sendai 980, Japan

(Received 19 July 1994)

We observed the interference effect of electron-capture x rays emitted by nuclear transformations in radioactive atoms. The interference fringes are generated between the direct monochromatic emissions from the radioactive atoms and the emissions totally reflected by the substrate surface. The site of a radioactive atom can be determined by analyzing the measured interference fringes because the period of these fringes depends on the position of the radioactive atoms relative to the substrate surface. A monolayer of ^{51}Cr above a Pt substrate was used as a model sample.

Element-selective positional information can be obtained by measuring the fluorescent yield or electron yield from the elements in an x-ray interference field, such as x-ray standing waves (XSW), in perfect single crystals,^{1,2} as well as XSW on substrate surfaces.³ In addition, the interference effect of secondary emissions from atoms has also been used to determine structural data, such as the Kossel pattern^{4,5} in perfect crystals, and fluorescent x-ray interference^{6,7} (FXI) in the above substrate surfaces.

Both the FXI fringes and the Kossel patterns show the angular distribution of fluorescent x rays emitted from an element. When this element is located in different sites in a sample, the FXI fringes and the Kossel patterns will show the sum of the fringes from many different sites. Thus, it is difficult to extract structural data on a specific site from the summation of patterns for all sites. Similarly, it is difficult to exact information on a particular site with conventional XSW experiments because only the summation of the fluorescent yield or electron yield is measured in XSW.

The method described in this paper can be used to distinguish between radioactive isotopes and radioinactive ones of the same element by using monochromatic radiations from radioactive atoms. In some experiments answers to physical or chemical questions can only be obtained through the use of radioactive atoms. Examples of this are the structural data for adsorbate-substrate interactions involving the same element, and self-diffusion in a solid or in a solution containing salts of the same element.

This paper reports on observations of the Lloyd's mirror-type⁸ interference effect in electron-capture x rays from radioactive atoms. We describe a method that uses interference patterns from radioisotopes (IPR) to obtain positional information about the radioactive atoms.

Here, we use Lloyd's mirror-type interference effect on monochromatic x rays from the radioactive atoms embedded in a noncrystalline material, as shown in Fig. 1. These monochromatic x rays are spontaneously emitted

from electron-capture-type radioactive atoms, for example, the K-electron capture in radioactive decay is accompanied by the emission of K x rays. X-ray emissions from a radioactive atom located above a substrate can take two optical paths: direct emission and totally reflected emission when the takeoff angle (θ_t) is smaller than the critical angle (θ_c) for total external reflection of x rays. The coherent sources are the primary source S_1 , which is the radioactive atom above a substrate, and its virtual image S_2 .

The optical path difference between the two sources depends on the distance (z) of the radioactive atom from the substrate and the phase shift that occurs at total reflection.⁹ Thus, positional information on the radioactive atoms can be obtained from the period of the observed interference fringes.

The theoretical interference pattern from the x-ray emissions can be calculated for a characteristic matrix of stratified media on the basis of reciprocity.¹⁰ In other words, the calculation of the characteristic x-ray intensity from coordinate z for takeoff angle θ_t is identical to that of the incident x-ray field at coordinate z for glancing angle θ_t . Although the emissions from radioisotopes have a

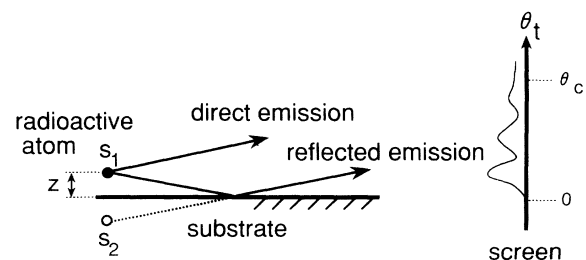


FIG. 1. Schematic of the interference phenomenon of the electron-capture x ray from a radioactive atom embedded within a sample. z represents the distance between the radioactive atom and the substrate surface. θ_t is the takeoff angle of the electron-capture x rays. The model interference fringes under θ_c is shown on the screen.

spherical wave form, a plane wave was observed under the conditions maintained for this experiment. This is because the distance between the observation point and the atomic source points is very long. Thus, the observed wave can be regarded as a plane wave, which is a component of a spherical wave.

When radioactive atoms act as characteristic x-ray sources with distribution N , the yield Y is given by

$$I(\theta_t, z) = |E_d + E_r|^2, \quad (1)$$

$$Y(\theta_t) = \int N(z)I(\theta_t, z)dz, \quad (2)$$

where $I(\theta_t, z)$ is the intensity of the characteristic x rays resulting from the interference effects between the direct and totally reflected emissions from coordinate z at the takeoff angle (θ_t). E_d and E_r are E -field plane waves for the direct and reflected emissions. $N(z)$ is the atom distribution at distance z from the substrate surface.

The sample we used in this experiment was a monoatomic ^{51}Cr layer deposited on an LB film on a Pt substrate. To separate radioisotopes from the substrate surface, we used an LB film made of a Pt substrate comprising a ^{51}Cr arachidate topmost monolayer and nine bilayers of cadmium arachidate, as shown in Fig. 2. The arachidic acid, was dissolved in chloroform (5×10^{-3} mol/l), was spread on the surface of the subphase at room temperature. The pH (6.5) of this subphase was adjusted with a 0.5-M sodium acetate buffer and 0.5-M NaOH. 50 μl of ^{51}Cr solution in the form of chromium chloride (CrCl_3) (Du Pont/Nemours & Co. Inc.) was suspended in the subphase and incubated at room temperature for about 2 h. The ^{51}Cr arachidate monolayer was transferred to the surface of the substrate ($10 \times 10 \text{ mm}^2$) at 40–45 mN/m by the horizontal dipping method. The distance z between the ^{51}Cr atoms and the surface of the Pt substrate was estimated to be 523 Å. Here, the thickness of the cadmium arachidate bilayer, as measured by x-ray diffraction was 55 Å, and the thickness of the Cr arachidate was assumed to be about 28 Å, which is ordinarily the case when the hydrocarbon chains are fully extended and untilted.

In this experiment, the specific radioactivity of ^{51}Cr atoms was 470 mCi/mg. We measured the total amount ($77 \pm 5 \text{ kBq}$) of the ^{51}Cr atoms transferred on the Pt substrate by counting the γ -ray peak area (320 keV) using a pure Ge detector (PGT Co.). The counting efficiency of the Ge detector was calibrated with ^{152}Eu and ^{241}Am standard sources. The total number of Cr atoms on the

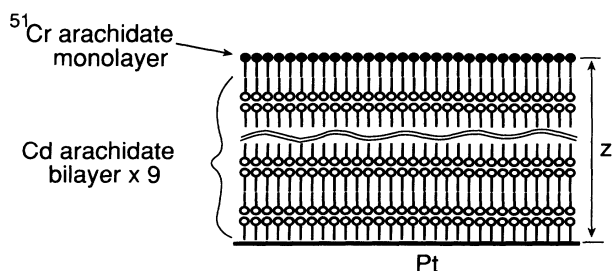


FIG. 2. Structure of the sample: Cross section of a monolayer of ^{51}Cr within LB film.

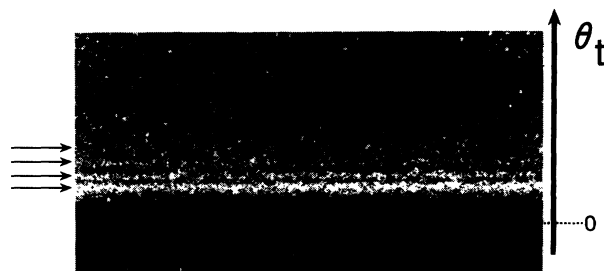


FIG. 3. Interference fringes of the electron-capture x-ray from the ^{51}Cr monolayer measured with the IP. The exposure time was 6 days. High-intensity areas of the measured x rays are shown by the arrows.

substrate was estimated to be $(5.2 \pm 0.3) \times 10^{13}$ atoms/cm². The number of metal atoms in the LB monolayer is usually about 10^{14} atoms/cm².¹¹ Thus, in this experiment the coating efficiency of the ^{51}Cr atoms was about 50% of the Cr arachidate monolayer.

To obtain an adequate signal-to-noise ratio for the monochromatic radiation from the ^{51}Cr atoms, we used a two-dimensional detector [an imaging plate¹² (IP)] as a wide-area detector. The IP is nonenergy dispersive and the ^{51}Cr emits vanadium $K\alpha$ (4.95 keV), vanadium $K\beta$ (5.42 keV), and γ ray (320 keV). Thus, the observed interference fringes were a mixture of V $K\alpha$, V $K\beta$, and γ rays. The γ rays (320 keV), however, were slightly absorbed through the Pt substrate. Thus, the intensity of the IP between -3 and zero mrad was defined as the background level necessary for subtracting the intensity of the γ rays and other background radiation. The distance from the sample to the detector was 300 mm. The IP detector size was about $127 \times 127 \text{ mm}$ (BAS-UR). The experiment was carried out in prepurified helium gas to reduce x-ray absorption, and in a 10-mm-thick Pb shield box to suppress background signals. The exposure times was 6 days. The IP was read out by a BAS-3000 system (Fuji Film Co.). The linearity of the IP was confirmed for Cu $K\beta$ and Mo $K\alpha$.

The interference fringes from ^{51}Cr measured with the IP are shown in Fig. 3. We measured three clear fringes. The sum of angular distribution from ^{51}Cr is shown in Fig. 4. The number of photons per pixel was calibrated using the x-ray intensity measured with a Si(Li) solid-state detector (Horiba. Co) with a rectangular slit ($50 \mu\text{m} \times 3.6 \text{ mm}$). The distance between the sample and the Si (Li) detector was 150 mm. We measured 6.7×10^{-3} counts/s (V $K\alpha$) at $\theta_t = 3.8 \text{ mrad}$. The statistical error for the experimental data in Fig. 4, defined by the square root of the estimated number of photons, corresponded to less than the diameter of the circle.

There were four fringes, as shown in Fig. 4: a first-order fringe at $\theta_t = 3.8 \text{ mrad}$, a second-order fringe at $\theta_t = 5.3 \text{ mrad}$, a third-order fringe at $\theta_t = 7.2 \text{ mrad}$, and a fourth-order fringe at $\theta_t = 9.1 \text{ mrad}$.

We calculated the theoretical interference fringes by χ^2 minimization fitting with Eq. (2). $N(z)$ is assumed to reach a maximum peak at $z = z_0$ and obey a Gaussian distribution with standard deviation σ . As a result of the χ^2

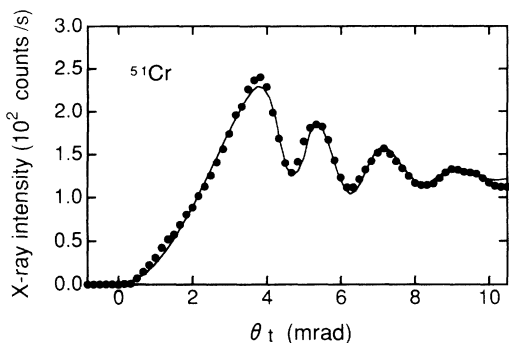


FIG. 4. Angular distribution (closed circles) of the integrated intensity along the fringes direction in Fig. 3. In theoretical fringes for the normalized yield, we used the following data: $z_0=486 \text{ \AA}$, $2\sigma=50 \text{ \AA}$, and the intensity ratio $V K\alpha/V K\beta$ is 7.0. The values of $1-(\text{the complex refractive indices})$ for LB film and Pt film (substrate): $(8.1+0.26i)\times 10^{-6}$, $(1.4+0.26i)\times 10^{-4}$, for $V K\alpha$, $(6.7+0.23i)\times 10^{-6}$, $(1.1+0.22i)\times 10^{-4}$, for $V K\beta$.

minimization fitting, we obtained a mean ^{51}Cr position of $z_0=486\pm 19 \text{ \AA}$ and a width of $2\sigma=50\pm 7 \text{ \AA}$. These values showed 63.8% data accuracy. The value of z_0 is smaller than what was the expected by 37 \AA , and the value 2σ was larger than the thickness (28 \AA) of the Cr

arachidate monolayer.

These results may be partially explained as follows. The surface of the ^{51}Cr monolayer was unstable in air because of its hydrophilicity. The ^{51}Cr monolayer may have undergone instantaneous reversal of orientation, known as overturning.¹³ If overturning partially occurred in the ^{51}Cr layer, the value 2σ may have been larger than that of the nonoverturned layer, and the value z_0 may have been shorter than what was expected.

In summary, we observed the interference fringes of electron-capture x rays from ^{51}Cr contained in an LB film. The distance between the ^{51}Cr atoms and the surface of the Pt substrate was obtained from the observed interference fringes of the electron-capture x rays. If radioactive and inactive atoms randomly occupy the same sites, there is no advantage of the IPR method. However, for instance, biological affinity reagents can specifically reacted with one of an amino acid in a potential.¹⁴

We would like to acknowledge valuable advice we received from Dr. A. Fukuhara. We are also grateful to Dr. T. Ido and K. Mori for providing the IP reader and IP plate, and M. Takahashi and S. Miura for their technical support in using the radioisotope, and S. Matsunami and N. Moriya for the LB through design.

¹B. W. Batterman, *Phys. Rev.* **133**, A759 (1964).

²S. K. Andersen, J. A. Golovchenko, and G. Mair, *Phys. Rev. Lett.* **37**, 1141 (1976); P. L. Cowan, J. A. Golovchenko, and M. F. Robbins, *Phys. Rev. Lett.* **44**, 1680 (1980).

³M. J. Bedzyk, G. M. Bommarito, and J. S. Schildkraut, *Phys. Rev. Lett.* **62**, 1376 (1989).

⁴W. Kossel, V. Loeck, and H. Voges, *Z. Phys.* **94**, 139 (1935).

⁵J. T. Hutton, G. T. Trammell, and J. P. Hannon, *Phys. Rev. B* **31**, 6420 (1985); T. Takahashi and M. Takahashi, *Jpn. J. Appl. Phys.* **32**, 5159 (1993).

⁶Y. C. Sasaki, Y. Suzuki, Y. Tomioka, and A. Fukuhara, *Phys. Rev. B* **48**, 7724 (1993).

⁷Y. C. Sasaki, Y. Suzuki, and T. Ishibashi, *Science* **263**, 62 (1994).

⁸W. Linnik, *Naturwissenschaften* **18**, 354 (1930); *Z. Phys.* **65**, 107 (1930).

⁹Y. Suzuki and S. Hasegawa, *Jpn. J. Appl. Phys.* **32**, 3261 (1993).

¹⁰M. Born and E. Wolf, *Principles of Optics*, 6th ed. (Pergamon, New York, 1980).

¹¹I. R. Peterson and G. J. Russel, *Philos. Mag. A* **49**, 463 (1984).

¹²J. Miyahara, K. Takahashi, Y. Amemiya, N. Kamiya, and Y. Satow, *Nucl. Instrum. Methods Phys. Res. Sect. A* **246**, 572 (1986).

¹³I. Langmuir, *Science* **87**, 493 (1938).

¹⁴B. L. Vallee and J. F. Riordan, *Ann. Rev. Biochem.* **38**, 733 (1969).

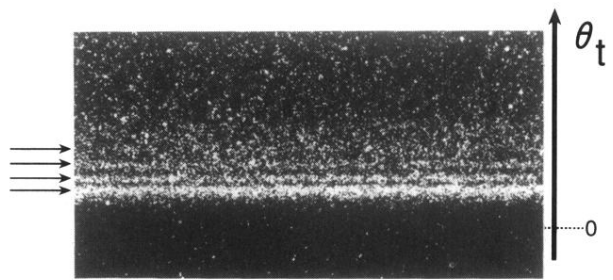


FIG. 3. Interference fringes of the electron-capture x ray from the ^{51}Cr monolayer measured with the IP. The exposure time was 6 days. High-intensity areas of the measured x rays are shown by the arrows.